scientific reports

Check for updates

OPEN

Mesenchymal stem cell-derived exosomes improve vascular remodeling by inhibiting EGFR/ErbB2 heterodimerization in hypoxic pulmonary hypertension

Yao-Xin Chen[1,4], Zhi-Hua Deng[1,4], Xiao-Wei She[2,4], Xue Gao[1], Xia-Ying Wei[1], Guo-Xing Zhang[3]✉ & Jin-Xian Qian[1]✉

A key characteristic of hypoxic pulmonary hypertension (HPH) is pulmonary vascular remodeling, involving abnormal proliferation and migration of pulmonary artery smooth muscle cells (PASMCs). Recent studies indicate that mesenchymal stem cell-derived exosomes (MSC-exo) exhibit therapeutic effects on HPH. MSC-exosomes were isolated from the conditioned medium of bone mesenchymal stem cells using ultracentrifugation, confirmed via Western blotting (WB), transmission electron microscopy (TEM), and nanoparticle tracking analyses (NTA). Platelet-derived growth factor BB (PDGFBB) induced pathological behavior in PASMCs, replicating the conditions observed in HPH. HPH rats were subjected to a low oxygen environment (10 ± 1% oxygen) for 8 h daily over 28 days. Parameters such as right ventricular systolic pressure (RVSP), right ventricular hypertrophy index (RVHI), and pulmonary vascular remodeling were evaluated. MSC-exosomes suppressed PDGFBB-induced proliferation and migration of PASMCs. Additionally, MSC-exosomes protected rats from hypoxia-induced increases in RVSP, right ventricular hypertrophy, and pulmonary vascular remodeling. The expression of epidermal growth factor receptor (EGFR) and Erb-B2 receptor tyrosine kinase 2 (ErbB2) was investigated in both HPH lung tissues and PDGFBB-induced PASMCs. Results indicated significant upregulation of EGFR/ErbB2 expression in HPH and PDGFBB-induced PASMCs, which was suppressed by MSC-exosomes. The study demonstrates that MSC-exosomes inhibit the development of HPH by suppressing excessive proliferation and migration of PASMCs through the inhibition of EGFR/ErbB2 heterodimerization.

Keywords Hypoxic pulmonary hypertension, Pulmonary vascular remodeling, Mesenchymal stem cell-derived exosomes, Epidermal growth factor receptor, Erb-B2 receptor tyrosine kinase 2

Hypoxic pulmonary hypertension (HPH) is a subset of pulmonary hypertension (PH) defined by the 6th World Symposium on Pulmonary Hypertension (WSPH)[1]. PH is classified into pre-capillary and post-capillary types. Pre-capillary PH is primarily caused by conditions such as pulmonary arterial disease, lung disease, hypoxia, chronic thromboembolism, or unknown etiologies. The WSPH Task Force has proposed defining abnormal pulmonary arterial pressure as a mean pulmonary arterial pressure (mPAP) greater than 20 mmHg. They also recommend including a pulmonary vascular resistance (PVR) threshold of at least 3 Wood Units in the definition of pre-capillary PH associated with mPAP > 20 mmHg, regardless of the underlying cause[1]. Hypoxia is a significant risk factor for pulmonary arterial hypertension (PAH), involving complex mechanisms contributing to pulmonary vascular remodeling[2–4]. Hypoxia can spark an inflammatory response and facilitate the release of inflammatory cytokines[5,6]. Additionally, it causes an overproduction of cytokines from contracting blood vessels,

[1]Department of Respiratory and Critical Care Medicine, Suzhou Municipal Hospital, Gusu School, The Affiliated Suzhou Hospital of Nanjing Medical University, Nanjing Medical University, Suzhou 215000, China. [2]Department of Thoracic Surgery, Suzhou Municipal Hospital, Gusu School, The Affiliated Suzhou Hospital of Nanjing Medical University, Nanjing Medical University, Suzhou 215000, China. [3]Department of Physiology and Neurosciences, Medical College of Soochow University, Suzhou 215000, China. [4]Yao-Xin Chen, Zhi-Hua Deng and Xiao-Wei She: These authors contributed equally to this work. ✉email: zhangguoxing@suda.edu.cn; qianjinxian@njmu.edu.cn

leading to increased vasoconstriction, pulmonary vascular resistance, and pulmonary artery pressure. Prolonged hypoxia can regulate the expression of pulmonary artery smooth muscle cell (PASMC) genes at a molecular level[4,7,8] resulting in pathological changes in the pulmonary vasculature, ultimately leading to right heart failure and mortality. Despite advancements in understanding the pathogenesis of HPH, identifying prognostic biomarkers, and developing treatment strategies, the incidence and mortality rates of HPH remain high[9,10]. Current therapies for pulmonary vasodilation primarily target the nitric oxide-cyclic guanosine monophosphate signaling pathway, enhance the effects of prostacyclin, or antagonize the endothelin pathway. However, these interventions may not always effectively treat HPH. For some patients with HPH, lung transplantation remains the only treatment option[11]. Given the controversies surrounding the efficacy of pulmonary vasodilator therapy, it is crucial to further understand the mechanisms underlying HPH development. This understanding can facilitate ongoing research and the development of more effective treatment strategies for HPH.

Mesenchymal stem cells (MSCs) possess multilineage differentiation potential, anti-inflammatory properties, and tissue repair capabilities[12,13]. These cells regulate inflammation and immune responses, differentiate into various cell types for tissue repair, and promote tissue regeneration[14]. Sourced from bone marrow, adipose tissue, and umbilical cord blood, MSCs are relatively accessible for research in various diseases[6,15]. However, direct use of MSCs carries risks such as immune rejection, chromosomal variations, and tumorigenic potential. Environmental factors can also influence MSCs' ability to home to damaged tissues, affecting their stability and efficiency[16]. To address these issues, research indicates that MSC culture supernatant or intracellular components can mediate biological functions, offering a more stable and efficient alternative. Focusing on secreted factors or components allows researchers to harness MSCs' therapeutic potential without the associated risks and challenges[12,16]. MSC-derived exosomes (MSC-exo) through paracrine signaling possess similar biological functions to MSCs and play a significant role in treating PH[16–18]. Previous studies have shown that exosomes derived from human umbilical cord mesenchymal stem cells improve pulmonary artery hypertension by inhibiting pulmonary vascular remodeling, which is highly inspiring for our research on hypoxic pulmonary hypertension[19]. Initially identified as a means of cellular communication, exosomes form through the budding of the cell membrane and contain a lipid bilayer structure similar to the plasma membrane. Their low immunogenicity makes them suitable for cell signaling and information exchange. Exosomes target recipient cells by binding to specific receptors on the cell membrane through receptor-ligand interaction or fusion, facilitating the transmission of biological information and exerting regulatory effects[16,17,20]. A key advantage of exosomes is their capacity to carry various biological molecules, enabling participation in different physiological and pathological processes[20–22]. In the context of PH, MSC-derived exosomes improve pulmonary vascular remodeling and reduce pulmonary artery pressure. They achieve this by inhibiting the proliferation of PASMCs, reducing endothelial cell apoptosis and migration, modulating the inflammatory response, and influencing the metabolic environment[6,15,21].

Erb-B2 receptor tyrosine kinase 2 (ErbB2), also known as human epidermal growth factor 2 (HER2), is a member of the EGF receptor family. Overexpressed in various cancer cells, ErbB2 plays a crucial role in tumor development, progression, and drug resistance mechanisms[23–27]. Ligand stimulation triggers homodimerization and heterodimerization among ErbB members, leading to receptor transphosphorylation and activation of downstream signals that promote cell growth, proliferation, differentiation, and migration[23,28]. Beyond tumor biology, ErbB2 is involved in other cellular processes[29] including vascular smooth muscle cell function. Under hypoxic conditions, EGFR and ErbB2 expression increases, contributing to the proliferation and fibrosis of these cells[30]. Emerging evidence suggests that miRNAs, such as miR-21, miR-221, and miR-486, have been shown to target EGFR or its downstream effectors directly, impacting the cellular response to EGFR activation[22]. Given the similarities between the abnormal proliferation of PASMCs in PH and tumor cells, it is hypothesized that ErbB2 may also participate in the pathological process of PH. MSC-exo may exert therapeutic effects in PH by reducing ErbB2 expression and inhibiting the formation of the EGFR/ErbB2 heterodimer, which is involved in cellular signaling pathways. Further research is imperative to fully understand the mechanisms underlying the therapeutic effects of MSC-exo in PH and their interactions with ErbB2.

Results

Preparation and characterization of exosomes derived from bone mesenchymal stem cells

The culture medium containing MSCs was successfully collected, and exosomes were extracted using ultracentrifugation and a concentration kit according to the manufacturer's instructions (Fig. 1A). To confirm the identity of the MSC-exo, several methods were employed. TEM determined the size and shape of the MSC-exo, revealing a range from 50 to 150 nm with a dish-like morphology. NTA further verified the size of the MSC-exo (Fig. 1B and C). Additionally, WB analysis detected specific protein markers (CD63, TSG101, and HSP90) known to be expressed in MSC-exo, with positive results (Fig. 1D). These characterized MSC-exo were then ready for subsequent experiments.

MSC-exo ameliorated PDGFBB-induced PASMC proliferation

Focusing on PASMC proliferation's role in pulmonary vascular remodeling in HPH, a PASMC proliferation model was established using PDGFBB, a potent mitogen and chemoattractant for vascular smooth muscle cells[31]. The Cell Counting Kit-8 (CCK-8) assay evaluated PASMC viability, showing increased absorbance at 450 nm with PDGFBB treatment, indicating enhanced cell viability. Introduction of MSC-exo reduced absorbance, suggesting inhibition of PASMC proliferation (Fig. 2A, $P < 0.01$). PASMC viability induced by PDGFBB peaked at 24 h compared to 48 and 72 h, thus selecting the 24-hour time point for further experiments.

WB analysis and immunofluorescence staining further investigated PASMC proliferation. Results indicated that PDGFBB treatment elevated the relative protein expression of PCNA and the percentage of Ki67-positive cells, signifying increased proliferation. Importantly, MSC-exo introduction significantly mitigated these

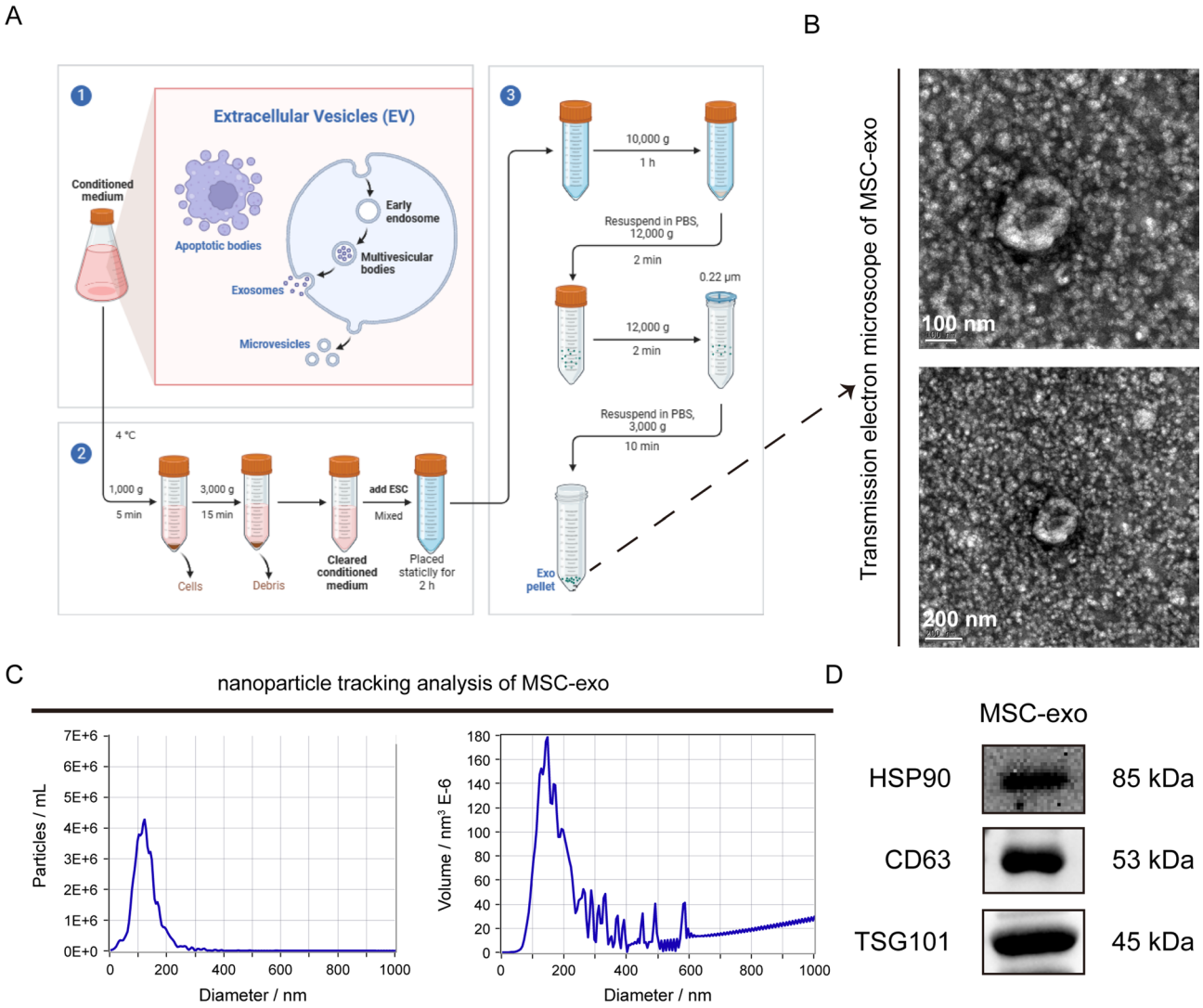

Fig. 1. Preparation and Characterization of Exosomes Derived from Bone Mesenchymal Stem Cells. **A**: Schematic diagram of MSC-exo extraction by ultracentrifugation; **B**: Shape of MSC-exo detected by TEM (Scale bar = 100–200 nm); **C**: Distribution of MSC-exo diameter and particles detected by NTA. **D**: Expression of MSC-exo protein markers analyzed by Western blotting; MSC-exo: exosome derived from mesenchymal stem cells; TEM: transmission electron microscopy; NTA: nanoparticle tracking analysis.

PDGFBB-induced changes, indicating that MSC-exo inhibits PDGFBB-induced PASMC proliferation (Fig. 2B and C, $P < 0.01$).

MSC-exo ameliorated PDGFBB-induced PASMC migration

Cell migration was next assessed using a wound-healing assay. Treatment with MSC-exo significantly reduced the percentage of wound closure following PDGFBB induction (Fig. 3A and B, $P < 0.001$), indicating that MSC-exo can effectively alleviate PDGFBB-induced PASMC proliferation and migration. By inhibiting both proliferation and migration, MSC-exo shows potential as a therapeutic approach to mitigate the effects of PDGFBB on PASMCs, potentially contributing to pulmonary vascular remodeling in the context of HPH.

EGFR/ErbB2 is highly expressed in PDGFBB-induced PASMCs

The role of HIF1α, EGFR, and ErbB2 in pulmonary vascular remodeling under hypoxic conditions and their modulation by MSC-exo was investigated. Firstly, HIF1α expression was found to be elevated in PDGFBB-induced PASMCs, while treatment with MSC-exo attenuated this expression (Fig. 4A, $P < 0.01$). To further explore the underlying mechanisms of MSC-exo in reversing HPH development, RT-qPCR was employed to determine the mRNA expression levels of EGFR and ErbB2 in PASMCs. The results showed significantly increased expression of both EGFR and ErbB2 in the PDGFBB-induced group compared to the normal group, while MSC-exo treatment effectively suppressed their expression levels (Fig. 4B and C, $P < 0.01$).

Immunofluorescence experiments revealed the colocalization of EGFR and ErbB2 in PASMCs following PDGFBB induction, with MSC-exo treatment reversing their expression (Fig. 4D). Additionally, WB analysis

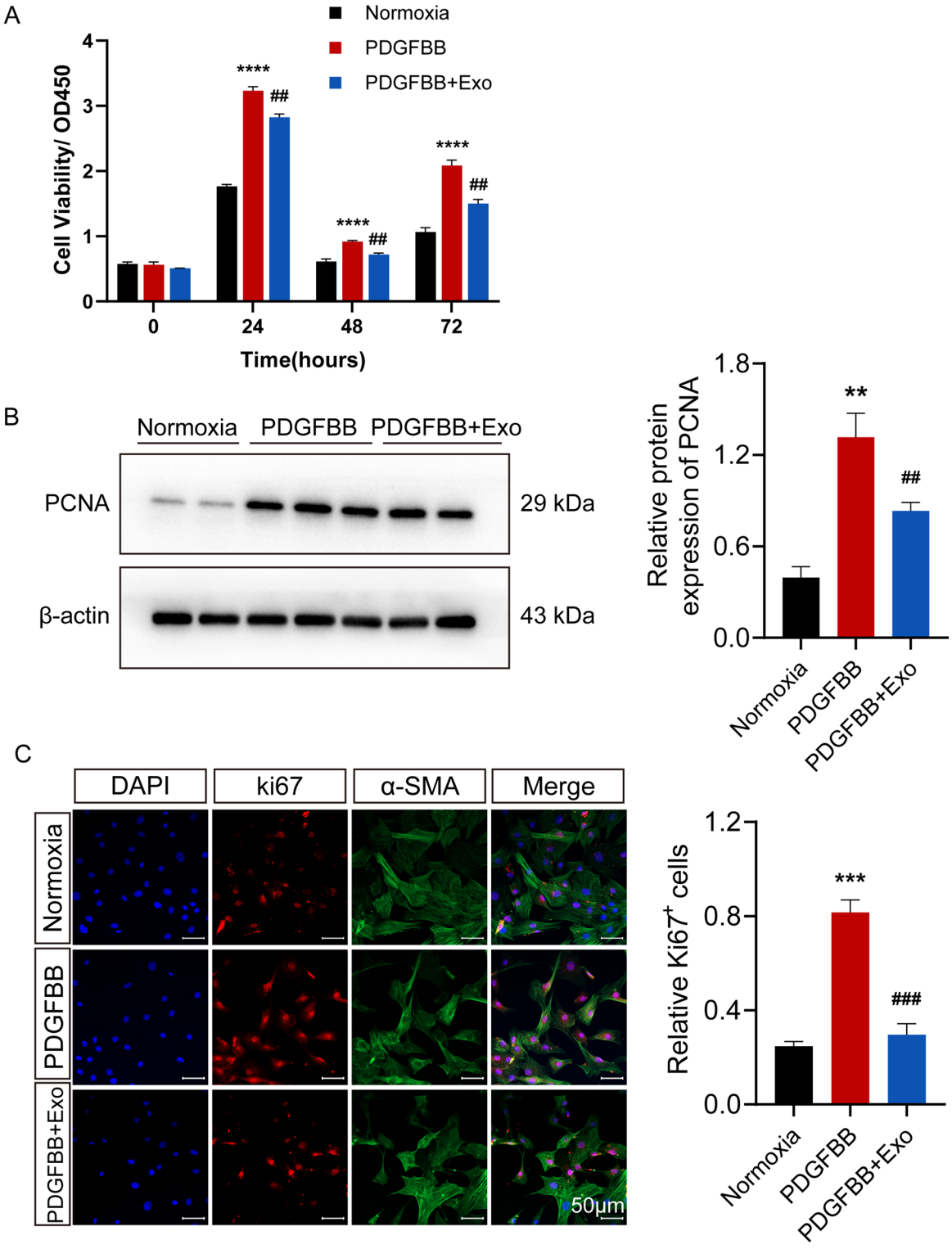

Fig. 2. MSC-exo Ameliorated PDGFBB-Induced PASMC Proliferation. **A**: Cell viability determined by CCK-8 analysis; **B**: Detection of PCNA protein expression by Western blotting analysis; **C**: Immunofluorescence staining of Ki67 in PASMC after co-incubation with PDGFBB for 24 h (Scale bar = 50 μm); ($n \geq 3$); Data are presented as mean ± SEM; **** indicates $P < 0.0001$, *** indicates $P < 0.001$, and ** indicates $P < 0.01$ for normoxia vs. PDGFBB. $^{\#\#\#\#}$ indicates $P < 0.0001$, $^{\#\#\#}$ indicates $P < 0.001$, and $^{\#\#}$ indicates $P < 0.01$ for MSC-exo vs. PDGFBB. PDGFBB: platelet-derived growth factor BB.

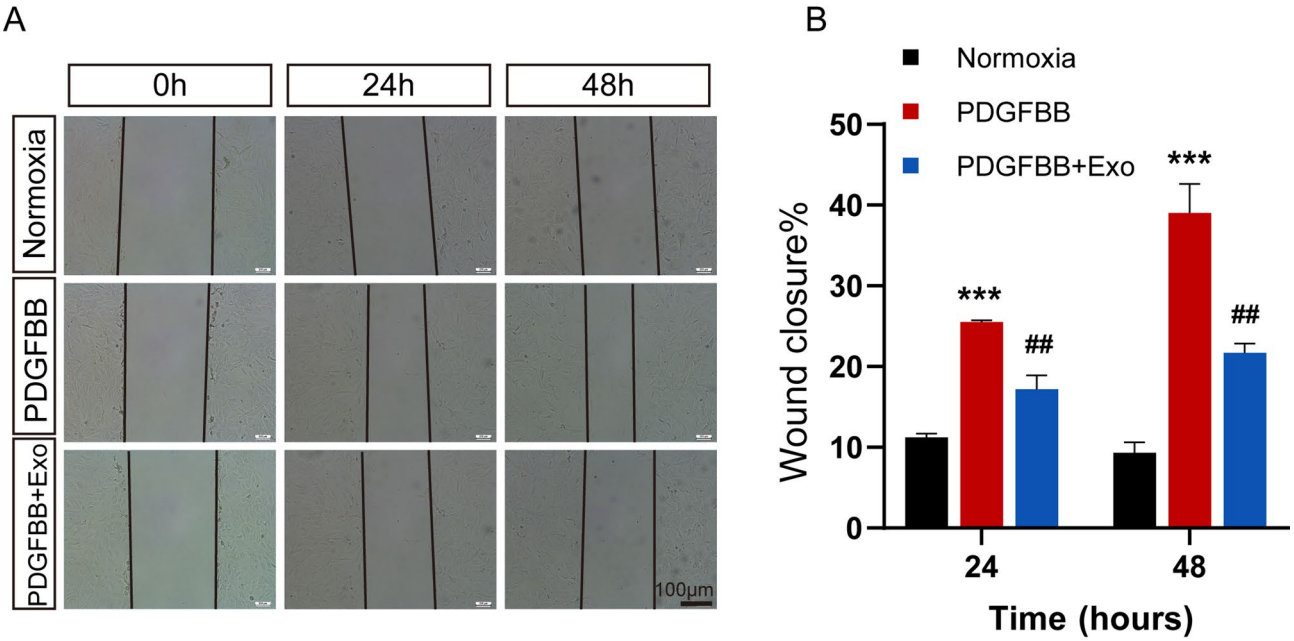

Fig. 3. MSC-exo Ameliorated PDGFBB-Induced PASMC Migration. **A**: Cell migration assessed by wound healing assay (Scale bar = 100 μm); **B**: Percentage of wound closure of PASMCs induced by PDGFBB at 24 h and 48 h; ($n \geq 3$); Data are presented as mean ± SEM; **** indicates $P < 0.0001$, *** indicates $P < 0.001$, and ** indicates $P < 0.01$ for normoxia vs. PDGFBB. #### indicates $P < 0.0001$, ### indicates $P < 0.001$, and ## indicates $P < 0.01$ for MSC-exo vs. PDGFBB.

demonstrated that MSC-exo inhibited the expression of ErbB2, which was elevated by PDGFBB (Fig. 4E, $P < 0.05$). These experimental results indicate that PDGFBB can induce the expression of HIF1α, EGFR, and ErbB2 in PASMCs and that their expression can be effectively inhibited by MSC-exo treatment. These findings enhance our understanding of the potential mechanisms underlying the beneficial effects of MSC-exo in mitigating pulmonary vascular remodeling associated with HPH.

MSC-exo reversed pulmonary vascular hypertrophy and thickening in HPH rats

This study aimed to investigate the therapeutic effect of MSC-exo on chronic HPH in rats. After 4 weeks of exposure to hypoxia (10% O_2), HPH rats were divided into two groups: one receiving MSC-exo injections and the other receiving PBS injections as a control, administered through the tail vein. The results demonstrated that RVSP was significantly higher in the hypoxia group compared to the normoxia group. However, RVSP was significantly lower in the MSC-exo group, indicating a beneficial effect of MSC-exo in reducing PH (Fig. 5A and B, $P < 0.0001$). Furthermore, histological examination of lung tissues using HE staining revealed that hypoxia led to an increase in the percentage of medial artery wall thickness and area, indicating thickening and hypertrophy of blood vessels in the HPH group. Treatment with MSC-exo reduced vessel thickening and hypertrophy in the HPH group (Fig. 5C and D, $P < 0.05$).

MSC-exo ameliorated the muscularization and fibrosis of peripheral pulmonary vessels in HPH rats

This study also examined the muscularization of peripheral pulmonary vessels and lung tissue fibrosis as key pathological changes in HPH. Immunohistochemical staining of lung sections using α-smooth muscle actin (α-SMA) as a marker for smooth muscle cells revealed that hypoxia-induced greater muscularization in peripheral pulmonary vessels compared to the normoxia group. However, MSC-exo treatment ameliorated this muscularization (Fig. 6A and B, $P < 0.01$). Additionally, lung tissue fibrosis was assessed using Masson's staining. The results showed an increase in the percentage of positively stained collagen volume, indicating fibrosis, in the HPH group. MSC-exo injections reduced the percentage of positively stained collagen volume, signifying a decrease in lung tissue fibrosis (Fig. 6C and D, $P < 0.05$). These findings further demonstrate that MSC-exo effectively protects against pulmonary vascular remodeling in HPH. The reduction in muscularization of peripheral pulmonary vessels and amelioration of lung tissue fibrosis highlight the potential therapeutic benefits of MSC-exo in attenuating pulmonary vascular remodeling associated with HPH.

MSC-exo suppressed right ventricular hypertrophy in HPH rats

Elevated pulmonary artery pressure leads to increased right ventricular afterload, causing right ventricular hypertrophy that gradually progresses to right ventricular failure, the leading cause of death in patients with HPH. This study aimed to investigate the effects of MSC-exo on right ventricular hypertrophy. Histological analysis of right ventricular muscle cells using HE staining demonstrated an increased CAS in the HPH group.

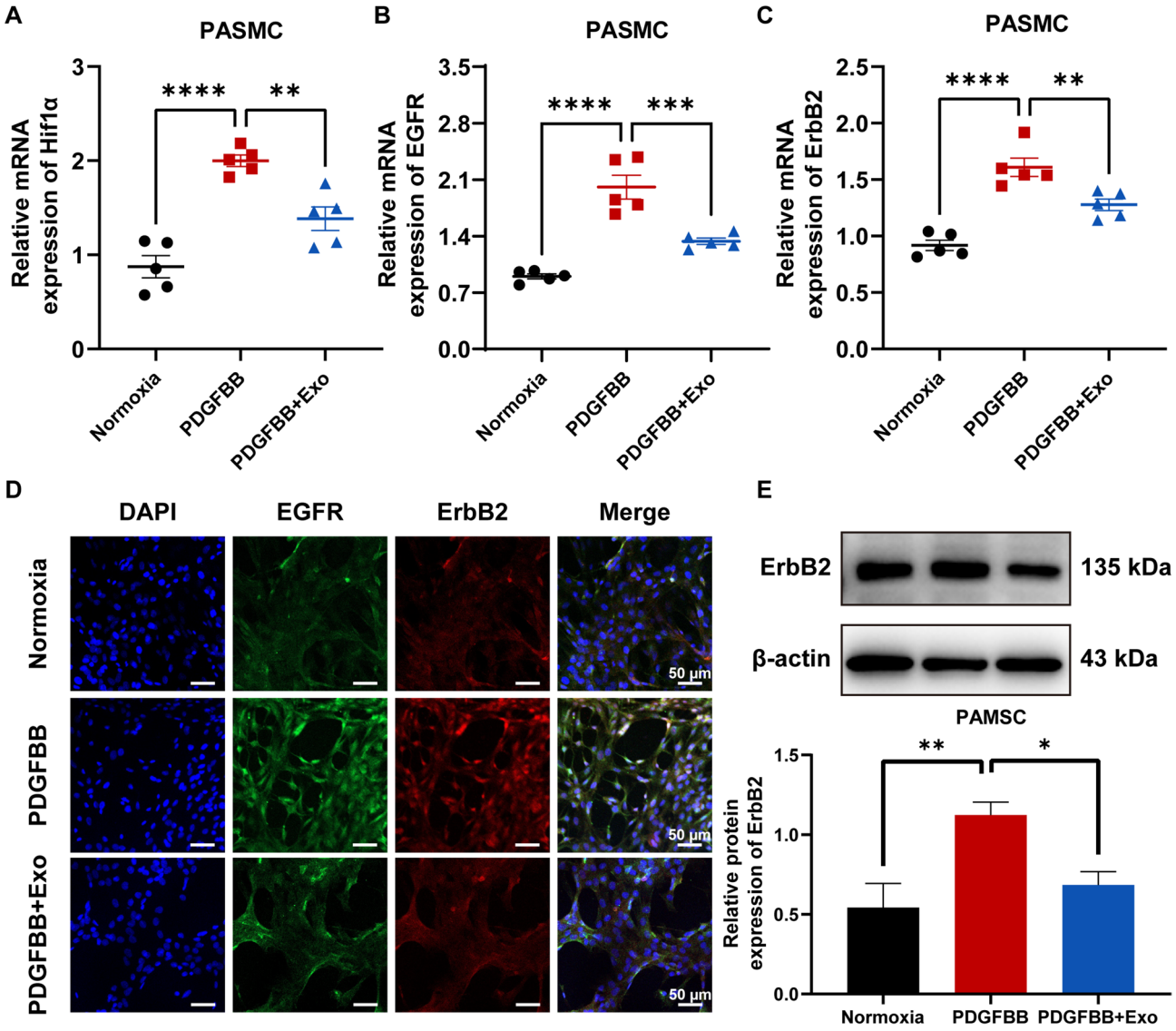

Fig. 4. EGFR/ErbB2 is Highly Expressed in PDGFBB-Induced PASMCs. **A-C**: RT-qPCR used to determine the mRNA expression of Hif1α, EGFR, and ErbB2 in PDGFBB-induced PASMCs; **D**: Immunofluorescence staining labeled EGFR and ErbB2 in PASMCs (Scale bar = 50 μm); **E**: Western blots used to determine the protein expression of ErbB2 in PASMCs; ($n \geq 3$); Data are presented as mean ± SEM; **** indicates $P < 0.0001$, *** indicates $P < 0.001$, ** indicates $P < 0.01$, and * indicates $P < 0.05$. EGFR: epidermal growth factor receptor; ErbB2: Erb-B2 receptor tyrosine kinase; Hif1α: hypoxia-inducible factor 1 subunit alpha.

However, MSC-exo treatment effectively reduced the CAS of these cells (Fig. 7A and B, $P < 0.01$). Additionally, Fulton's index, the ratio of right ventricle to left ventricle plus septum (RV/LV + S), was evaluated as a measure of right ventricular hypertrophy. The results indicated that MSC-exo treatment reversed the increase in Fulton's index induced by chronic hypoxia (Fig. 7C, $P < 0.001$). These findings suggest that MSC- exo has an anti-hypertrophy effect on right ventricular hypertrophy in HPH rats, indicating its potential as a therapeutic strategy for attenuating the development of right ventricular hypertrophy and its associated complications in HPH.

MSC-exo depressed high expression of EGFR/ErbB2 in HPH rats

This study investigated the effect of MSC-exo on the activity of EGFR/ErbB2 in PASMCs during vascular remodeling, building on our previous findings. To explore these effects at the tissue level, WB analysis was performed to assess the expression levels of HIF1α, EGFR, and ErbB2. The results showed that hypoxia induced an increase in the expression of HIF1α, EGFR, and ErbB2. However, treatment with MSC-exo inhibited the expression of these proteins (Fig. 8, $P < 0.05$). These findings suggest that hypoxia induces the upregulation of the EGFR/ErbB2 heterodimer, which contributes to pulmonary vascular remodeling during the development of PH. The administration of MSC-exo counteracts this effect by inhibiting the expression of the EGFR/ErbB2 heterodimer.

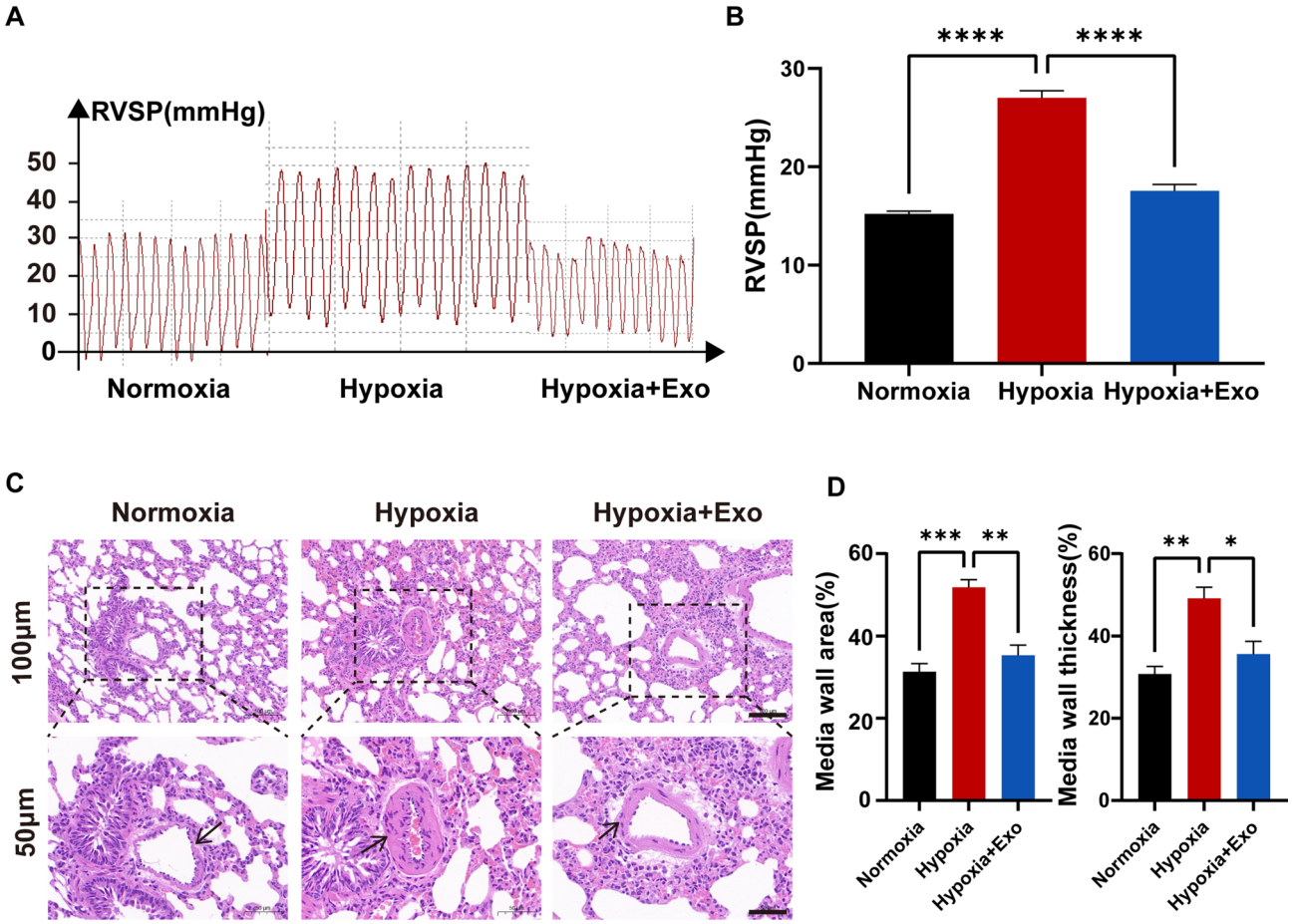

Fig. 5. MSC-exo Reversed Pulmonary Vascular Hypertrophy and Thickening in Chronic Hypoxic Pulmonary Hypertension Rats. **A-B**: Measurement of RVSP and the real-time detected pressure waveform; **C**: Representative lung sections stained with hematoxylin-eosin (Scale bar = 100 μm–50 μm); **D**: Measurement of medial arterial wall area and thickness of distal pulmonary vessels; ($n \geq 3$); Data are presented as mean ± SEM; **** indicates $P < 0.0001$, *** indicates $P < 0.001$, ** indicates $P < 0.01$, and * indicates $P < 0.05$. RVSP: right ventricular systolic pressure.

Discussion

This study demonstrated that MSC-exo suppressed PDGFBB-induced PASMC proliferation, migration, and EGFR/ErbB2 expression in vitro. Additionally, MSC-exo treatment significantly reduced RVSP, inhibited pulmonary vascular and right ventricular remodeling, and decreased EGFR/ErbB2 expression in HPH rats. HPH is a severe complication in chronic hypoxic lung diseases, such as chronic obstructive pulmonary disease (COPD)[1,4,32]. Falling under the third category of pulmonary hypertension, PH treatment options, including clinical vascular expansion treatments, still remain controversial[10,11]. Currently, there is no cure for PH, and in severe cases, lung transplantation may be the only option[9]. Consequently, the mortality rate for PH remains high. The progression of elevated pulmonary artery pressure increases right ventricular afterload, ultimately leading to right ventricular failure, the primary cause of death in patients with PH. Chronic hypoxia plays a significant role in the development of PH by triggering pulmonary vascular remodeling[2,3]. This remodeling process involves endothelial cell injury, abnormal proliferation and migration of PASMCs, and the accumulation of extracellular matrix fibrous tissue and collagen. Imbalances between cellular apoptosis and proliferation, along with excessive extracellular matrix deposition, contribute to pulmonary vascular remodeling[33–35]. Systemic hypoxia also induces erythropoietin (EPO) expression, increasing hematocrit and pulmonary vascular resistance[4]. Furthermore, hypoxia regulates gene expression, influencing cellular responses involved in developing HPH. Studies have shown the involvement of various factors, such as long non-coding RNA CASC2, in vascular remodeling in HPH[36,37]. Interestingly, research has demonstrated that (MSC-exo) can exert therapeutic effects on PH. Exosomes, effective carriers of biological factors secreted by MSCs, are distinguished from microvesicles[6,14,15].

The epidermal growth factor (EGF) receptor, a member of the receptor tyrosine kinase (RTK) superfamily, includes ErbB1/EGFR/HER1, ErbB2/Neu/HER2, ErbB3/HER3, and ErbB4/HER4[28]. At least 12 ligands, such as EGF, heparin-binding EGF-like growth factor (HB-EGF), epiregulin (Epi), transforming growth factor-α (TGF-α), and neuregulins can activate the ErbB receptor family[29]. Ligand stimulation triggers

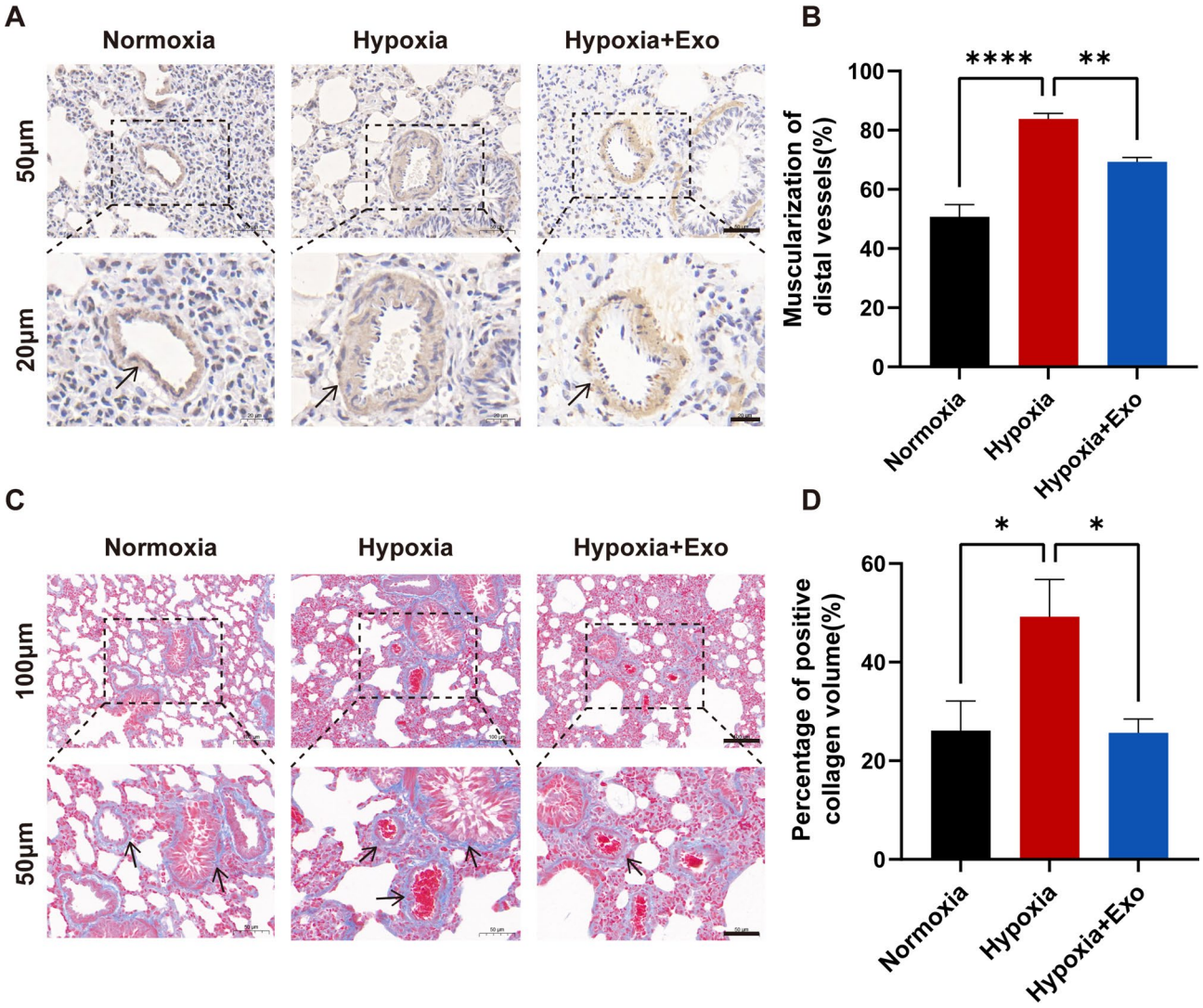

Fig. 6. MSC-exo Ameliorated the Muscularization and Fibrosis of Peripheral Pulmonary Vessels in HPH Rats. **A**: Immunohistochemical staining for α-SMA in peripheral pulmonary vessels and representative images of terminal pulmonary vessels (Scale bar = 50 μm–20 μm); **B**: Percentage of muscularization in distal pulmonary vessels; **C**: Representative lung sections stained with Masson's stain and the percentage of positive collagen volume (Scale bar = 100 μm–50 μm); **D**: Percentage of positive collagen volume in distal pulmonary vessels; ($n \geq 3$); Data are presented as mean ± SEM; **** indicates $P < 0.0001$, ** indicates $P < 0.01$, and * indicates $P < 0.05$. α-SMA: α-smooth muscle actin.

homodimerization and heterodimerization among ErbB members, leading to receptor transphosphorylation and activation of downstream signals that promote cell growth, proliferation, differentiation, and migration[38–40]. Altered expression of EGF ligands and ErbB receptors is linked to various cancers, including breast, esophageal, colorectal, and cervical cancer.

The EGFR-ErbB2 heterodimer demonstrates greater stability than the EGFR-EGFR homodimer[41]and ErbB2 overexpression enhances EGFR signaling. Combined inhibition of EGFR and ErbB2 more effectively suppresses tumor growth than blocking either receptor alone[23,25]. Recent studies have explored the EGF family in non-neoplastic diseases. For example, patients with obstructive ventilatory sleep disorders show elevated expression of EGF family receptors, particularly ErbB2, in vascular smooth muscle cells in response to intermittent hypoxic stimulation. This elevation stimulates smooth muscle cell proliferation and migration, contributing to atherogenesis[30]. Hypoxia also alters the EGF system in human hearts, with HER2 downregulation suppressing cardiomyocyte proliferation under hypoxic conditions[29].

Given these findings, it is speculated that EGFR/ErbB2 heterodimer expression similarly increases during smooth muscle cell hyperproliferation in PH. The protective effect of MSC-exo against HPH may be achieved by inhibiting EGFR/ErbB2 expression. As excessive proliferation and migration of PASMCs under hypoxia conditions are essential processes leading to pulmonary vascular remodeling in PH, the pathological cell behavior of PASMCs undergoing abnormal proliferation and migration was established using PDGFBB

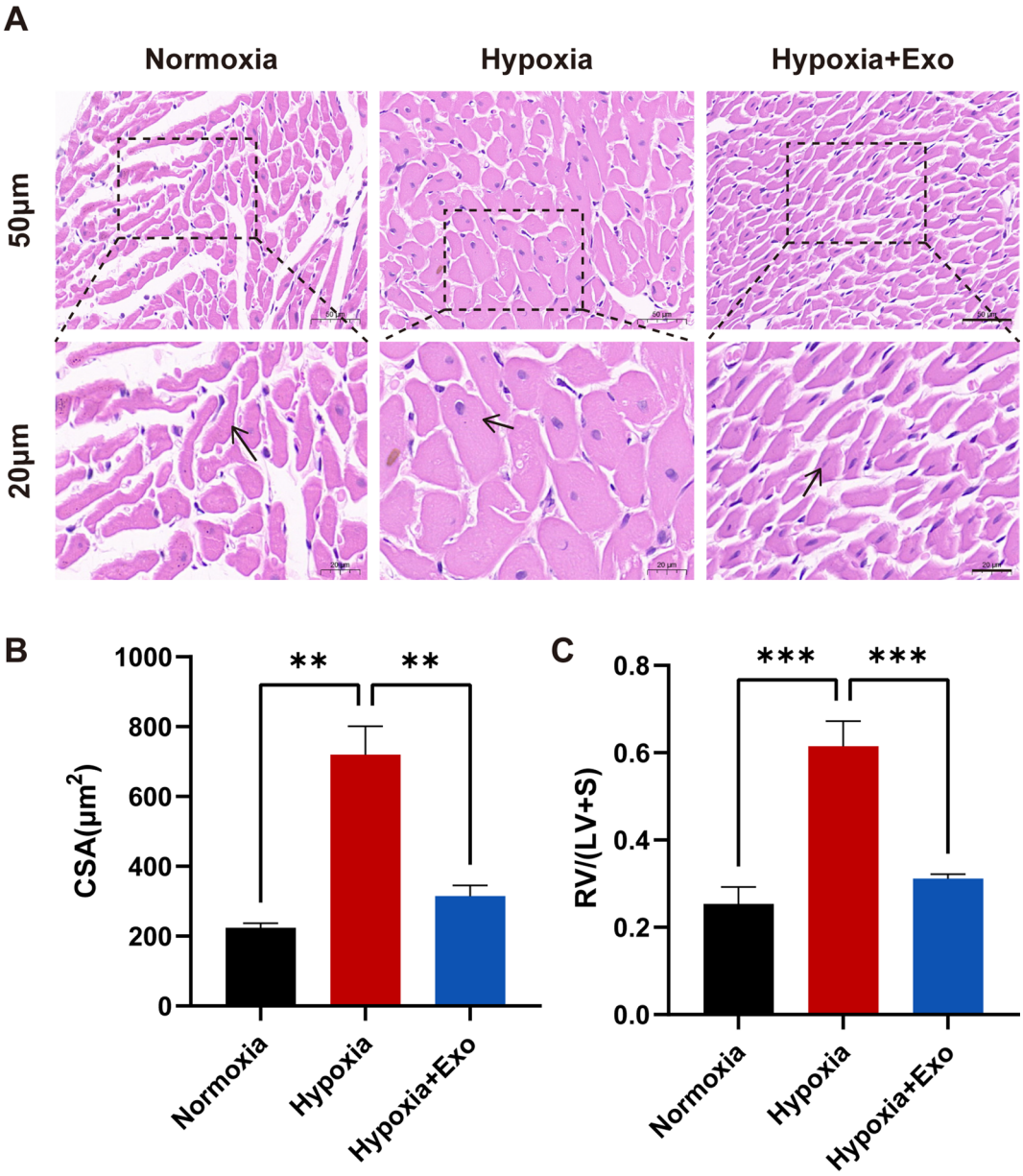

Fig. 7. MSC-exo Suppressed Right Ventricular Hypertrophy in HPH Rats. **A**: Representative images of H&E staining of the right ventricular muscle cell (Scale bar = 50 μm–20 μm); **B**: Percentage of single cell cross-sectional area; ($n \geq 3$); **C**: Ratio of RV/LV + S, indicating the degree of right ventricular hypertrophy; Data are presented as mean ± SEM; *** indicates $P < 0.001$ and ** indicates $P < 0.01$. RV/LV + S: right ventricle / left ventricle plus septum.

induction. PDGFBB is a strong mitogen that can promote the abnormal proliferation and migration of PASMCs, and it has been shown to be one of the important mediators involved in the development of HPH. Our experiments demonstrated that PDGFBB induction increased cell viability and enhanced the proliferation and migration abilities of cells. WB results from our study showed elevated ErbB2 expression in hypoxia cell models induced by PDGFBB, and ErbB2 expression was significantly decreased after co-culture with MSC-exo. Additionally, immunofluorescence analysis results showed that EGFR/ErbB2 expression was increased under PDGFBB stimulation and could also be suppressed by MSC-exo, indicating that they might form heterodimers to regulate HPH.

An HPH rat model was constructed for in vivo experiments. Rats in the HPH group were exposed to hypoxic conditions for 8 h daily over 28 days, with oxygen concentration maintained at 10 ± 1% by filling with nitrogen. After 28 days, hemodynamic measurements and pathological analyses of heart and pulmonary tissues were performed. Compared to normoxic rats, hypoxic rats exhibited a significant increase in right ventricle systolic pressure (RVSP), an indirect indicator of pulmonary arterial pressure. HE staining showed thickened vascular walls and narrowed lumens in the distal pulmonary arteries of HPH rats. Additionally, increased

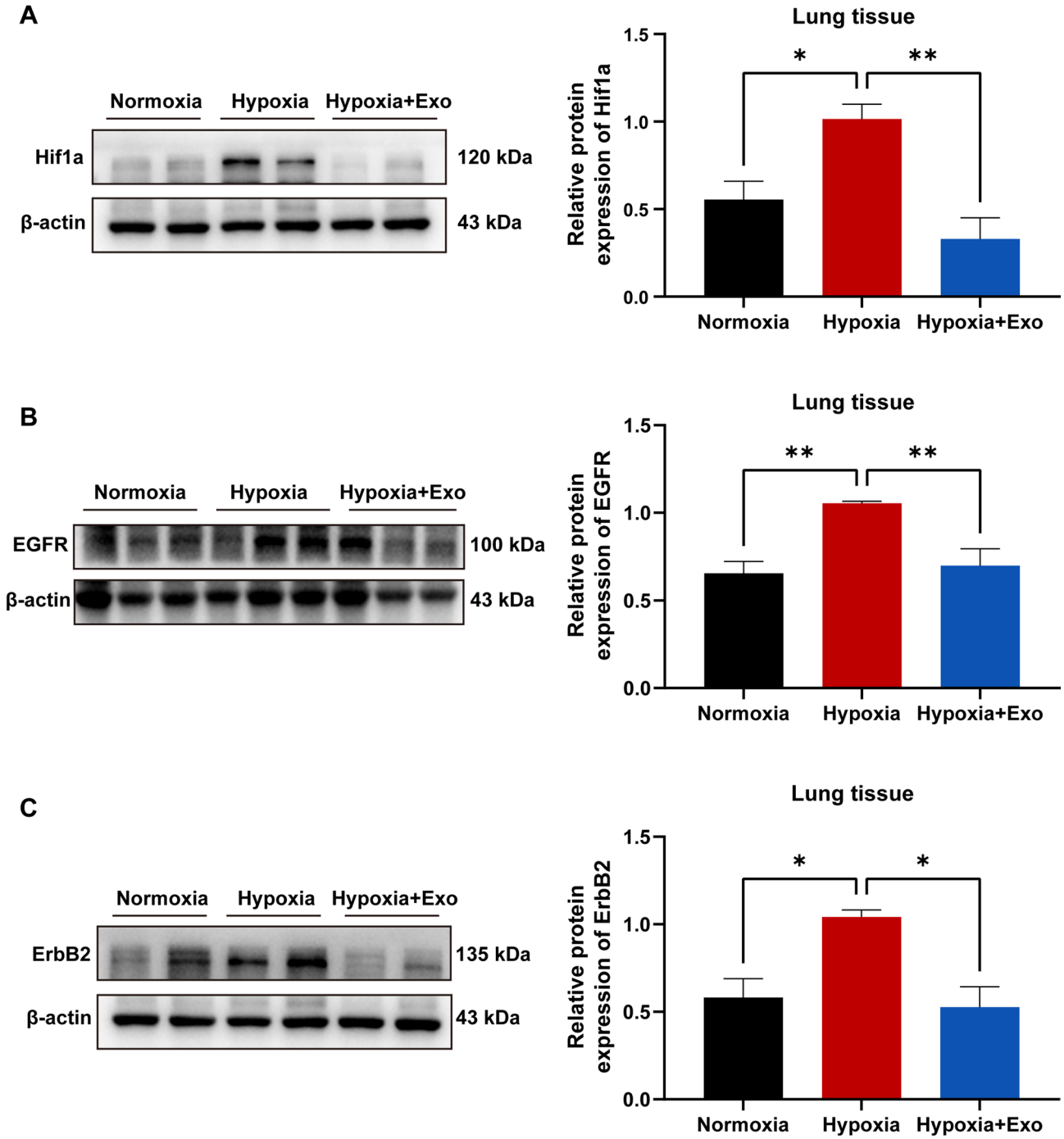

Fig. 8. EGFR/ErbB2 Pathway is Highly Expressed in HPH Rats. **A**: Western blots used to determine the protein expression of Hif1α in lung tissue; **B**: Western blots used to determine the protein expression of EGFR in lung tissue; **C**: Western blots used to determine the protein expression of ErbB2 in lung tissue; ($n \geq 3$); Data are presented as mean ± SEM; ** indicates $P < 0.01$ and * indicates $P < 0.05$.

muscularization and fibrosis of peripheral pulmonary vessels were observed, indicating pulmonary vascular remodeling in HPH rats. These findings confirm the successful establishment of the HPH rat model. MSC-exo and PBS vehicle were then injected into HPH rats three times weekly for three weeks. The results demonstrated a reversal of the increased RVSP and a reduction in distal pulmonary arterial remodeling in HPH rats treated with MSC-exo. Moreover, the right ventricular muscle hypertrophy index, significantly increased by hypoxia, was alleviated following MSC-exo intervention. These findings suggest a protective effect of MSC-derived exosomes against HPH. Importantly, elevated EGFR/ErbB2 expression was detected in HPH lung tissues, with decreased expression following MSC-exo injection.

Previous studies have demonstrated that Hif1α is up-regulated in HPH[42,43]our research has also confirmed it. Meanwhile, in oncological studies, potential targets related to underlying mechanisms are identified through the construction and analysis of protein-protein interaction (PPI) networks, Hif1α, EGFR, and ERBB2 have all been recognized as key hub targets. The interactions among these targets suggest potential functional associations in the mechanism of tumors[44]. Moreover, Hif1α plays a crucial role in ERBB2 (HER2/neu)-mediated proliferation of breast cancer cells[27]. ERBB2 stabilizes Hif1α and activates its downstream signaling pathways, significantly promoting cell proliferation and maintaining tumor growth[27]. Conversely, the absence of Hif1α leads to a marked decrease in the proliferative capacity of ERBB2-positive tumor cells, highlighting Hif1α as a key regulator of ERBB2-mediated proliferation[27]. Therefore, we believe that Hif1α is highly correlated with the expression and functional effects of EGFR/ErbB2.

Collectively, these results indicate that the elevated expression of EGFR/ErbB2 heterodimers promotes PASMC proliferation and migration, contributing to pulmonary vascular remodeling and the development of PH. MSC-exo may exert a protective effect on HPH by inhibiting the expression of EGFR/ErbB2 heterodimers. Hif-1α may be involved in the formation and functional activity of the EGFR/ERBB2 heterodimer.

In conclusion, our results confirm the therapeutic protective effect of MSC-exo on HPH and identify the EGFR/ErbB2 heterodimer as a key mediator in this process by regulating PASMC proliferation and migration. Targeting the EGFR/ErbB2 heterodimer may represent a potential therapeutic strategy for HPH. A better understanding of its upstream regulators and downstream mechanisms is crucial for designing innovative therapies for HPH. Future research will focus on these areas to develop more effective treatments.

Materials and methods

Extraction of exosomes from human bone marrow mesenchymal stem cells

Human bone marrow-derived mesenchymal stem cells were generously provided by the Hematology Research Institute of the First Affiliated Hospital of Soochow University, as previously demonstrated in our earlier studies[45]. They were cultured in media supplemented with human platelet lysate (StemCell, USA, #05439) to prevent any exosome contamination from fetal bovine serum. Once cell confluence attained 80–90%, the culture medium was collected and exosomes isolated by ultracentrifugation. Briefly, Exosome Concentration Solution (Umibio, Shanghai, China, #UR52111) was added to the cultured medium and incubated at 4 °C for 2 h. The mixture was then centrifuged at 10,000 g for 60 min, followed by discarding the supernatant, and the precipitate was resuspended in PBS and centrifuged again at 12,000 g for 2 min. This step was repeated until no significant precipitate remained. The collected supernatant was filtered through an Exosome Purification Filter (Umibio, Shanghai, China, #UR90102) and then centrifuged at 3,000 g for 10 min. The purified exosomes were collected and stored at -80 °C. Protein concentration was determined using a BCA Assay Kit (Beyotime, Shanghai, China, #P0010). Western blotting (WB) analysis with antibodies specific to CD63, TSG101, and HSP90 validated the immunophenotype of the exosomes. Furthermore, transmission electron microscopy (TEM) and nanoparticle tracking analysis (NTA) were employed to examine the size and morphology of MSC-derived exosomes (MSC-exo). The identified MSC-exo was then used for subsequent experiments.

Animal experiment and hemodynamic measurements

Thirty adult male Sprague Dawley (SD) rats, with a weight range of 180 to 220 g, were obtained from the Experimental Animal Center of Soochow University (Jiangsu, China) and housed in a specific pathogen-free (SPF) facility. The rats were randomly divided into three groups ($n = 10$): normoxia, hypoxia, and hypoxia with MSC-exo treatment. The normoxic group was exposed to normal atmospheric oxygen levels (21%), while the hypoxia group was exposed to low oxygen levels ($10 \pm 1\%$) for 8 h daily over 28 days. The intermittent hypoxia protocol effectively induced key features of HPH, such as elevated pulmonary artery pressure, vascular remodeling, and right ventricular hypertrophy, as shown by our previous data[46]. To maintain the desired oxygen concentration, a hypoxia chamber (Nanjing Xingfei Analytical Instruments, Nanjing, China, #XF-2CL) was ventilated with nitrogen, and carbon dioxide, water vapor, and ammonia were removed using an air pump.

After 4 weeks, the rats with HPH were removed from the hypoxic condition. Half of these rats ($n = 10$) were then tail intravenously injected with MSC-exo at a dosage of 100 μg protein per kg of body weight once daily for 3 days per week over 3 weeks. The remaining HPH rats ($n = 10$) received an equal volume of PBS as a control group using the same injection method. After 3 weeks, the rats were anesthetized with isoflurane. Subsequently, the rats were immobilized and implanted with a polystyrene PE-50 catheter (Bunzl Healthcare, London, UK) through the right jugular vein. One end of the catheter was placed into the right ventricle and secured, while the other end was connected to a heart performance analysis system (Alcott Biotech, Shanghai, China). The setup featured a pressure sensor to measure RVSP in real-time after pressure stabilization. Similarly, the carotid artery pressure was assessed. Finally, the rats were euthanized via intraperitoneal injection of an overdose of pentobarbital (150–200 mg/kg), and their heart and lung tissues were harvested for subsequent experiments.

Histology analysis of lung sections

Histopathological examination of lung sections assessed pulmonary artery remodeling. Entire lung lobes were fixed in 4% paraformaldehyde, embedded in paraffin, and sliced into 5 μm sections. Hematoxylin-eosin (HE) staining was performed on the prepared sections, followed by microscopic observation (Olympus, Tokyo, Japan) and image collection. Media thickness (WT = outer diameter - inner diameter), outer diameter (ED), tube wall area, and lumen area were calculated to evaluate vessel wall thickening. The percentage of media thickness (WT%) was calculated as (WT / ED) × 100%, and the percentage of media area (WA%) as (tube wall area/lumen area) × 100%. Additionally, immunohistochemical staining of paraffin-embedded sections with α-smooth muscle actin (α-SMA; 1:100, Abcam, USA, #ab7817) primary antibody assessed the degree of muscularization of peripheral pulmonary vessels.

Measurement of right ventricle hypertrophy

Rat hearts were harvested, and the right ventricle free wall (RV), left ventricle, and septum (LV + S) were isolated and weighed. To evaluate right ventricular hypertrophy, the ratio of RV to LV + S weight (RV/LV + S) was calculated. Myocardial tissue was stained with HE, and the cross-sectional area (CAS%) of individual ventricular muscle cells was measured to assess cardiac hypertrophy.

Pulmonary artery smooth muscle cell (PASMC) culture and hypoxic induction

Primary PASMCs were extracted from the pulmonary arteries of SD male rats aged 2–3 weeks and cultured in an incubator set at 37 °C with a 5% CO_2 atmosphere. The culture medium was composed of 90% high-glucose Dulbecco's modified Eagle's medium (DMEM) (Gibco, Germany, #C11995), 10% fetal bovine serum (FBS) (Gibco, Germany, #10099-141), as well as penicillin (100 U/mL), and streptomycin (100 mg/mL). PASMCs were passaged upon reaching 80% confluence, with passage 3–6 cells used for all experiments. Before experimentation, cells were serum-starved for 24 h and then divided into three groups: normoxia (21% O_2, 5% CO_2, 74% N_2); hypoxia with PDGFBB treatment (20 ng/mL DMEM); and hypoxia with PDGFBB (20 ng/mL DMEM) and MSC-exo (100 μg protein/mL DMEM). During the modeling experiment, all groups were cultured in a medium without serum.

Cell viability and proliferation analysis

The viability of PASMCs cultured with PDGFBB and MSC-exo was assessed using a Cell Counting Kit-8 assay (Glpbio, USA, #GK10001). Cells were seeded in 96-well plates at a density of 5×10^3 cells/well under standard culture conditions. Upon reaching over 70% confluence, cells were starved for 24 h and then treated with PDGFBB for 24 and 48 h, with or without MSC-exo. After treatment, cells were incubated with CCK8 solution (10 μL/well) for 2 h, and absorbance at 450 nm was measured using a microplate reader. Protein expression of proliferating cell nuclear antigen (PCNA) and Ki67 immunofluorescence staining in PASMCs were analyzed to evaluate cell proliferation.

Cell migration assay

The migratory ability of PASMCs was assessed using a wound healing assay. Cells were seeded in 6-well plates and treated as previously described. Upon reaching 90–100% confluence, three straight scratches were made in the cell layer using a 200 μL pipette tip. Representative images of PASMCs were taken at specified time points using a microscope (Olympus, Tokyo, Japan). Cell migration was quantified by measuring the reduction in scratch width.

Western blotting analysis

WB analysis detected the relative expression of target proteins in each sample. Total protein was extracted from prepared lung tissue, PASMC, and MSC-exo samples using RIPA buffer (Beyotime, China, #P0013C) with 1% PMSF (Beyotime, China, #ST506) and protease inhibitor. The lysate buffer was added to the samples, lysed on ice for 30 min, sonicated, and centrifuged at 12,000 g for 15 min at 4 °C, and the supernatant was collected as the protein sample. Protein concentration was determined using a BCA assay, followed by preparation of the corresponding protein loading system. Extracted protein underwent SDS-PAGE separation and transfer onto PVDF membranes (Millipore, USA). Membranes were rinsed with TBS-T, blocked with 5% non-fat milk for 2 h at room temperature, then incubated overnight at 4 °C with primary antibodies: anti-CD63 (1:1000; ImmunoWay, USA, #YT5525), anti-HSP90 (1:1000; Abways, Shanghai, China, #CY5181), anti-TSG101 (1:1000; Abcam, USA, #ab125011), anti-PCNA (1:2000; Abcam, USA, #ab29), anti-Hif1α (1:2000; ImmunoWay, USA, #YT2133), anti-EGFR (1:2000; ImmunoWay, USA, #YT1497), anti-ErbB2 (1:2000; Proteintech, China, #18299-1-AP), and anti-β-actin (1:5000; Abways, USA, #AY0573). The following day, membranes were washed and incubated with HRP-conjugated anti-rabbit or mouse IgG (1:5000, Beyotime, Shanghai, China, #A0216) for 1 h at room temperature. Enhanced chemiluminescent (ECL) reagent (R&D Systems, USA) visualized the membrane blot, followed by exposure to the Thermo image analysis system (Bio-Rad, USA). ImageJ software (Rawak Software, Germany) analyzed the blot. Relative protein expression was determined by the gray value ratio of protein bands to β-actin, serving as an internal control to normalize protein levels.

Quantitative realtime PCR

Extract total RNA from PASMCs and convert it into complementary DNA (cDNA) using reverse transcription kits (RR036A, Takara, Japan). Prepare the qPCR reaction mix using the TB Green Premix Ex Taq II kit (Tli RNaseH Plus) (RR820A, Takara, Japan). Perform the qPCR amplification on the LightCycler 480 instrument, following the manufacturer's protocol. β-actin served as the housekeeping gene for normalization. The relative expression of the target genes was quantified employing the $2^{-\Delta\Delta Ct}$ method. Primers were synthesized by Azenta Life Sciences Biotech (Suzhou, China). The primers for each target gene were as follows: rat Hif1α: forward 5'-CCATCAGTTACTTACGTGTG-3', reverse 5'-ACCATAACAAAGCCATCCAG-3'; rat EGFR: forward 5'-AAGACCACTTTCTGAGCCTCC-3', reverse 5'-GAACATAGCCAGCCACCTCC-3'; rat ErbB2: forward 5'-CCCGAGACTGATGGCTATGT-3', reverse 5'-AACCCCATTCTTCCCAGGAG-3'; rat β-actin: forward 5'-GGAGATTACTGCCCTGGCTCCTAGC-3', reverse 5'-GGCCGGACTCATCGTACTCCTGCTT-3';

Immunofluorescence staining

PASMCs cultured on slides were fixed with 4% paraformaldehyde for 15 min. After washing with PBS three times, cells were permeabilized with 0.1% Triton X-100. Slides were blocked with 0.1% BSA for 30 min at room temperature, followed by incubation with primary antibodies against EGFR and ErbB2 at 4 °C overnight. The slides were then incubated with Goat Anti-Rabbit IgG Alexa Fluor 594 or 488 (1:500, Abways, China) for 60 min

at room temperature. Nuclei were stained with 4′,6-Diamidino-2-phenylindole (DAPI). Observations and image capture were performed using a fluorescence microscope (Olympus, Tokyo, Japan).

Statistical analysis

Statistical analyses were conducted using GraphPad Prism (version 9.0) software. At least three independent replicates were performed, and data were presented as mean ± standard error of the mean (SEM). Data conforming to normal distribution and homogeneity of variance were analyzed using one-way ANOVA; otherwise, Welch's correction was applied. A *P*-value of less than 0.05 was considered statistically significant.

Data availability

The datasets used and/or analysed during the current study available from the corresponding author on reasonable request.

Received: 3 December 2024; Accepted: 26 June 2025
Published online: 07 July 2025

References

1. Galie, N., McLaughlin, V. V., Rubin, L. J. & Simonneau, G. An overview of the 6th World Symposium on Pulmonary Hypertension. *Eur. Respir. J.* **53**, (2019). https://doi.org/10.1183/13993003.02148-2018
2. Lucero Garcia Rojas, E. Y., Villanueva, C. & Bond, R. A. Hypoxia inducible factors as central players in the pathogenesis and pathophysiology of cardiovascular diseases. *Front. Cardiovasc. Med.* **8**, 709509. https://doi.org/10.3389/fcvm.2021.709509 (2021).
3. Yang, L., Liang, H., Shen, L., Guan, Z. & Meng, X. LncRNA Tug1 involves in the pulmonary vascular remodeling in mice with hypoxic pulmonary hypertension via the microRNA-374c-mediated Foxc1. *Life Sci.* **237**, 116769. https://doi.org/10.1016/j.lfs.2019.116769 (2019).
4. Waypa, G. B. & Schumacker, P. T. Roles of HIF1 and HIF2 in pulmonary hypertension: it all depends on the context. *Eur. Respir. J.* **54** https://doi.org/10.1183/13993003.01929-2019 (2019).
5. Li, Y. et al. MicroRNA-150 relieves vascular remodeling and fibrosis in hypoxia-induced pulmonary hypertension. *Biomed. Pharmacother.* **109**, 1740–1749. https://doi.org/10.1016/j.biopha.2018.11.058 (2019).
6. Lee, C. et al. Exosomes mediate the cytoprotective action of mesenchymal stromal cells on hypoxia-induced pulmonary hypertension. *Circulation* **126**, 2601–2611. https://doi.org/10.1161/CIRCULATIONAHA.112.114173 (2012).
7. Mandras, S. A., Mehta, H. S. & Vaidya, A. Pulmonary hypertension: A brief guide for clinicians. *Mayo Clin. Proc.* **95**, 1978–1988. https://doi.org/10.1016/j.mayocp.2020.04.039 (2020).
8. Zhang, L. et al. Blockade of JAK2 protects mice against hypoxia-induced pulmonary arterial hypertension by repressing pulmonary arterial smooth muscle cell proliferation. *Cell. Prolif.* **53**, e12742. https://doi.org/10.1111/cpr.12742 (2020).
9. Thenappan, T., Ormiston, M. L., Ryan, J. J. & Archer, S. L. Pulmonary arterial hypertension: pathogenesis and clinical management. *BMJ* **360**, j5492. https://doi.org/10.1136/bmj.j5492 (2018).
10. Vonk Noordegraaf, A., Groeneveldt, J. A. & Bogaard, H. J. Pulmonary hypertension. *Eur. Respir Rev.* **25** https://doi.org/10.1183/16000617.0096-2015 (2016).
11. Ruopp, N. F. & Cockrill, B. A. Diagnosis and treatment of pulmonary arterial hypertension: A review. *JAMA* **327**, 1379–1391. https://doi.org/10.1001/jama.2022.4402 (2022).
12. Pittenger, M. F. et al. Mesenchymal stem cell perspective: cell biology to clinical progress. *NPJ Regen Med.* **4** https://doi.org/10.1038/s41536-019-0083-6 (2019).
13. Wen, Z. et al. Mesenchymal stem cell-derived exosomes ameliorate cardiomyocyte apoptosis in hypoxic conditions through microRNA144 by targeting the PTEN/AKT pathway. *Stem Cell. Res. Ther.* **11**, 36. https://doi.org/10.1186/s13287-020-1563-8 (2020).
14. Aliotta, J. M. et al. Exosomes induce and reverse monocrotaline-induced pulmonary hypertension in mice. *Cardiovasc. Res.* **110**, 319–330. https://doi.org/10.1093/cvr/cvw054 (2016).
15. Klinger, J. R. et al. Mesenchymal stem cell extracellular vesicles reverse sugen/hypoxia pulmonary hypertension in rats. *Am. J. Respir Cell. Mol. Biol.* **62**, 577–587. https://doi.org/10.1165/rcmb.2019-0154OC (2020).
16. Yu, B., Zhang, X. & Li, X. Exosomes derived from mesenchymal stem cells. *Int. J. Mol. Sci.* **15**, 4142–4157. https://doi.org/10.3390/ijms15034142 (2014).
17. Zhang, J. et al. Exosome and Exosomal microrna: trafficking, sorting, and function. *Genomics Proteom. Bioinf.* **13**, 17–24. https://doi.org/10.1016/j.gpb.2015.02.001 (2015).
18. Yang, S. et al. Every road leads to rome: therapeutic effect and mechanism of the extracellular vesicles of human embryonic stem cell-derived immune and matrix regulatory cells administered to mouse models of pulmonary fibrosis through different routes. *Stem Cell. Res. Ther.* **13**, 163. https://doi.org/10.1186/s13287-022-02839-7 (2022).
19. Zhang, S. et al. Mesenchymal stromal cell-derived exosomes improve pulmonary hypertension through Inhibition of pulmonary vascular remodeling. *Respir. Res.* **21** https://doi.org/10.1186/s12931-020-1331-4 (2020).
20. Mohan, A., Agarwal, S., Clauss, M., Britt, N. S. & Dhillon, N. K. Extracellular vesicles: novel communicators in lung diseases. *Respir Res.* **21**, 175. https://doi.org/10.1186/s12931-020-01423-y (2020).
21. Hogan, S. E. et al. Mesenchymal stromal cell-derived exosomes improve mitochondrial health in pulmonary arterial hypertension. *Am. J. Physiol. Lung Cell. Mol. Physiol.* **316**, L723–L737. https://doi.org/10.1152/ajplung.00058.2018 (2019).
22. Wang, R., Xu, Y., Tong, L., Zhang, X. & Zhang, S. Recent progress of Exosomal lncRNA/circRNA–miRNA–mRNA axis in lung cancer: implication for clinical application. *Front. Mol. Biosci.* **11** https://doi.org/10.3389/fmolb.2024.1417306 (2024).
23. Balz, L. M. et al. The interplay of HER2/HER3/PI3K and EGFR/HER2/PLC-γ1 signalling in breast cancer cell migration and dissemination. *J. Pathol.* **227**, 234–244. https://doi.org/10.1002/path.3991 (2012).
24. Liu, H. et al. Erb–B2 receptor tyrosine kinase 2 is negatively regulated by the p53–responsive microRNA–3184–5p in cervical cancer cells. *Oncol. Rep.* **45** https://doi.org/10.3892/or.2020.7862 (2021).
25. Reid, A., Vidal, L., Shaw, H. & de Bono, J. Dual Inhibition of ErbB1 (EGFR/HER1) and ErbB2 (HER2/neu). *Eur. J. Cancer.* **43**, 481–489 (2007).
26. Chen, Y. et al. Erb-b2 receptor tyrosine kinase 2 (ERBB2) promotes ATG12-Dependent autophagy contributing to treatment resistance of breast Cancer cells. *Cancers (Basel).* 13. https://doi.org/10.3390/cancers13051038 (2021).
27. Whelan, K. A. et al. The oncogene HER2/neu (ERBB2) requires the hypoxia-inducible factor HIF-1 for mammary tumor growth and Anoikis resistance. *J. Biol. Chem.* **288**, 15865–15877. https://doi.org/10.1074/jbc.M112.426999 (2013).
28. Zhan, L., Xiang, B. & Muthuswamy, S. K. Controlled activation of ErbB1/ErbB2 heterodimers promote invasion of three-dimensional organized epithelia in an ErbB1-dependent manner: implications for progression of ErbB2-overexpressing tumors. *Cancer Res.* **66**, 5201–5208. https://doi.org/10.1158/0008-5472.CAN-05-4081 (2006).

29. Munk, M. et al. Hypoxia changes the expression of the epidermal growth factor (EGF) system in human hearts and cultured cardiomyocytes. *PLoS One*. **7**, e40243. https://doi.org/10.1371/journal.pone.0040243 (2012).
30. Kyotani, Y. et al. Intermittent hypoxia induces the proliferation of rat vascular smooth muscle cell with the increases in epidermal growth factor family and erbB2 receptor. *Exp. Cell. Res.* **319**, 3042–3050. https://doi.org/10.1016/j.yexcr.2013.08.014 (2013).
31. Tannenberg, P. et al. Extracellular retention of PDGF-B directs vascular remodeling in mouse hypoxia-induced pulmonary hypertension. *Am. J. Physiol. Lung Cell. Mol. Physiol.* **314**, L593–L605. https://doi.org/10.1152/ajplung.00054.2017 (2018).
32. Sockrider, M. What is pulmonary hypertension?? *Am. J. Respir Crit. Care Med.* **203**, P12–P13. https://doi.org/10.1164/rccm.2035P12 (2021).
33. Evans, C. E., Cober, N. D., Dai, Z., Stewart, D. J. & Zhao, Y. Y. Endothelial cells in the pathogenesis of pulmonary arterial hypertension. *Eur. Respir. J.* **58** https://doi.org/10.1183/13993003.03957-2020 (2021).
34. Ranchoux, B. et al. Endothelial-to-mesenchymal transition in pulmonary hypertension. *Circulation* **131**, 1006–1018. https://doi.org/10.1161/CIRCULATIONAHA.114.008750 (2015).
35. Zhao, L. et al. The zinc transporter ZIP12 regulates the pulmonary vascular response to chronic hypoxia. *Nature* **524**, 356–360. https://doi.org/10.1038/nature14620 (2015).
36. Wang, J. et al. Decoding CeRNA regulatory network in the pulmonary artery of hypoxia-induced pulmonary hypertension (HPH) rat model. *Cell. Biosci.* **12**, 27. https://doi.org/10.1186/s13578-022-00762-1 (2022).
37. Gong, J. et al. Long non-coding RNA CASC2 suppresses pulmonary artery smooth muscle cell proliferation and phenotypic switch in hypoxia-induced pulmonary hypertension. *Respir Res.* **20**, 53. https://doi.org/10.1186/s12931-019-1018-x (2019).
38. Li, L. Y. et al. Nuclear ErbB2 enhances translation and cell growth by activating transcription of ribosomal RNA genes. *Cancer Res.* **71**, 4269–4279. https://doi.org/10.1158/0008-5472.CAN-10-3504 (2011).
39. Ebbing, E. A. et al. Esophageal adenocarcinoma cells and xenograft tumors exposed to Erb-b2 receptor tyrosine kinase 2 and 3 inhibitors activate transforming growth factor Beta signaling, which induces epithelial to mesenchymal transition. *Gastroenterology* **153** https://doi.org/10.1053/j.gastro.2017.03.004 (2017).
40. Hynes, N. E. ErbB2: from an EGFR relative to a central target for Cancer therapy. *Cancer Res.* **76**, 3659–3662. https://doi.org/10.1158/0008-5472.CAN-16-1356 (2016).
41. Motamedi, Z. & Rajabi-Maham, H. Azimzadeh irani, M. Glycosylation promotes the cancer regulator EGFR-ErbB2 heterodimer formation - molecular dynamics study. *J. Mol. Model.* **27**, 361. https://doi.org/10.1007/s00894-021-04986-9 (2021).
42. Wan, J. J., Yi, J., Wang, F. Y., Zhang, C. & Dai, A. G. Expression and regulation of HIF-1a in hypoxic pulmonary hypertension: focus on pathological mechanism and Pharmacological treatment. *Int. J. Med. Sci.* **21**, 45–60. https://doi.org/10.7150/ijms.88216 (2024).
43. Liu, J. et al. IL-33 initiates vascular remodelling in hypoxic pulmonary hypertension by up-Regulating HIF-1α and VEGF expression in vascular endothelial cells. *EBioMedicine* **33**, 196–210. https://doi.org/10.1016/j.ebiom.2018.06.003 (2018).
44. Rajadnya, R. et al. Novel systems biology experimental pipeline reveals matairesinol's antimetastatic potential in prostate cancer: an integrated approach of network pharmacology, bioinformatics, and experimental validation. *Brief. Bioinform.* **25** https://doi.org/10.1093/bib/bbae466 (2024).
45. Chen, Y. X. et al. Exosomes derived from mesenchymal stromal cells exert a therapeutic effect on hypoxia-induced pulmonary hypertension by modulating the YAP1/SPP1 signaling pathway. *Biomed. Pharmacother.* **168** https://doi.org/10.1016/j.biopha.2023.115816 (2023).
46. Deng, Z. H. et al. Mesenchymal stem cell-derived exosomes ameliorate hypoxic pulmonary hypertension by inhibiting the Hsp90aa1/ERK/pERK pathway. *Biochem. Pharmacol.* **226** https://doi.org/10.1016/j.bcp.2024.116382 (2024).

Acknowledgements
none.

Author contributions
Chen Y.X. : Investigation, Methodology, Visualization, and Writing - original draft. Deng Z.H. and She X.W. : Data curation, Formal analysis, and Investigation. Gao X. and Wei X.Y. : Validation and Visualization. Zhang G.X. : Project administration, Supervision, and Writing - review & editing. Qian J.X. : Conceptualization, Funding acquisition, and Writing - review & editing. All authors reviewed the manuscript.

Funding
This work was supported by the Gusu Talent Cultivation Project of Health (GSWS2019061).

Declarations

Competing interests
The authors declare no competing interests.

Ethics statement
All animal experiments received approval from the Animal Ethics Committee of Soochow University (20220201A0303) and were conducted according to their established guidelines. The use of animals and experimental procedures strictly adhered to international ethical standards and the National Institutes of Health's guidelines for the care and use of laboratory animals. Our research involving live animals is conducted in accordance with the ARRIVE guidelines.

Additional information
Supplementary Information The online version contains supplementary material available at https://doi.org/10.1038/s41598-025-09333-z.

Correspondence and requests for materials should be addressed to G.-X.Z. or J.-X.Q.